Journal of the Serbian Chemical Society
JSCS-info@shd.org.rs • www.shd.org.rs/JSCS
J. Serb. Chem. Soc. *82* (10) 1175–1191 (2017)
JSCS–5032
UDC 628.161.2:546.19'48'815+
541.183:546.723–31–36:539.12
Original scientific paper

Removal of heavy metals from water using multistage functionalized multiwall carbon nanotubes

DRAGOSLAV BUDIMIROVIĆ[1], ZLATE S. VELIČKOVIĆ[2], ZORAN BAJIĆ[2], DRAGANA L. MILOŠEVIĆ[3], JASMINA B. NIKOLIĆ[1]*[#], SAŠA Ž. DRMANIĆ[1#] and ALEKSANDAR D. MARINKOVIĆ[1#]

[1]*Faculty of Technology and Metallurgy, University of Belgrade, Karnegijeva 4, 11120 Belgrade, Serbia,* [2]*Military Academy, University of Defense, generala Pavla Jurišića-Šturma 33, Belgrade, Serbia and* [3]*Institute of Chemistry, Technology and Metallurgy, University of Belgrade, Njegoševa 12, Belgrade ,Serbia*

(Received 22 April, revised 29 May, accepted 29 May 2017)

Abstract: The multistage synthesis of the multi-wall carbon nanotubes (MWCNT) modified with polyamidoamine dendrimers, A1/ and A2/MWCNT, capable of cation removal, is presented in this work, as well as novel adsorbents based on these precursor materials and modified with goethite nano-deposit, *α*-FeOOH, A1/ and A2/MWCNT–*α*-FeO(OH) adsorbents used for As(V) removal. In a batch test, the influence of pH, contact time, initial ion concentration and temperature on adsorption efficiency were studied. Adsorption data modelling by the Langmuir isotherm, revealed good adsorption capacities (in mg g^{-1}) of 18.8 for As(V) and 60.1 and 44.2 for Pb^{2+} and Cd^{2+} on A2/MWCNT, respectively. Also, 27.6 and 29.8 mg g^{-1} of As(V) on A1/ and A2/MWCNT–*α*-FeO(OH), respectively, were removed. Thermodynamic parameters showed that the adsorption is spontaneous and endothermic processes. Results of the study of influences of competitive ions: bicarbonate, sulfate, phosphate, silicate, chromate, fluoride and natural organic matter (NOM), *i.e.*, humic acid (HA), showed the highest effect of phosphate on the decrease of arsenate adsorption. Time-dependent adsorption was best described by pseudo-second-order kinetic model and Weber–Morris model which predicted intra-particle diffusion as a rate-controlling step. Also, activation energy (E_a / kJ mol^{-1}): 8.85 for Cd^{2+}, 9.25 for Pb^{2+} and 7.98 for As(V), were obtained from kinetic data.

Keywords: arsenic; cadmium; lead; adsorption; nanocomposites; MWCNT; goethite.

* Corresponding author. E-mail: jasmina@tmf.bg.ac.rs
[#] Serbian Chemical Society member.
https://doi.org/10.2298/JSC170422066B

Available on line at www.shd.org.rs/JSCS/
(CC) 2017 SCS.

INTRODUCTION

Arsenic, cadmium and lead are among the heavy metals which the World Health Organization designated as particularly harmful to human health and hence influenced the legislation of many countries to reduce their level of maximum permissible concentration. According to the recommendations of the World Health Organization, the maximum permissible concentration of these metals (mg L^{-1}) in drinking water for arsenic is limited to 0.01, for cadmium to 0.003 and for lead to 0.01. Low restrictive boundaries for these heavy metals have imposed a challenging problem in the control of environmental pollution. A wide range of water treatment technologies such as chemical precipitation, ion exchange, membrane filtration, and adsorption may be used for the removal of heavy metals, but these methods of water treatment still suffer from some inherent limitations. Chemical precipitation, the traditional method that is commonly used to remove heavy metals from contaminated sources, is often associated with the generation of large amounts of sludge, and also has limitations for the removal of heavy metals only at low but illicit concentrations. The process of ion exchange is a process that generally relates to the treatment or removal of heavy metals at low concentrations. In membrane filtration, the main problems are sedimentation of dirt and membrane breakage which entail high maintenance costs. Taking all this into consideration, adsorption is one of the most rewarding and the most commonly used methods in the study of new materials and the conditions for the removal of heavy metals from water.[1–7]

Development and application of new nanostructured materials, including carbon nanotubes, in the field of water treatment has enabled the development of various combinations of modification and functionalization in order to synthesize a high-capacity adsorbents with the possibility of multiple applications, minimal environmental impact and also to satisfy profitability regarding their possible use. Regardless of enormous effort performed by scientific community directed toward this goal, the published results did not provide satisfactory technology/material which could satisfy established criteria.[6–11]

According to numerous studies, adsorption is strongly influenced by the pH value of the solution, because it affects the adsorbate solubility and its concentration, the concentration of adsorbent functional groups and adsorbate ionization in solution. In addition, properties of the adsorbent, specific surface area, pore volume and size, point of zero charge and functionalities could have significant influence on the adsorption process.[6,9,12,13]

Presented study is a continuation of the research of high-performance adsorbents based on multi-wall carbon nanotubes (MWCNT) intended for heavy metals removal. The synthesis of adsorbents is carried out in controlled multistage introduction of significant number of terminal amino group[14] on A1/ and A2/MWCNT adsorbents, applicable for Cd^{2+} and Pb^{2+} as well as As(V) oxyanion

(CC) 2017 SCS.

removal. The subsequent modification by controlled precipitation of iron(oxy)-hydroxide in the form of goethite produced A1/ and A2/MWCNT–α-FeO(OH) is useful for arsenate removal.[9,15] The obtained adsorbents were characterized using BET, SEM and FTIR techniques along with the determination of the pH values of the point of zero charge. The results of adsorption investigations are discussed from the point of the time of adsorption, pH value of the solution, adsorbent mass, temperature and the influences of competitive ions.

EXPERIMENTAL

Materials

All the chemicals used in this study were of analytical grade and used as received. The following chemicals were supplied from Sigma-Aldrich: raw-MWCNT (purity >95%), tetrahydrofurane (THF), ethylenediamine (EDA), ethyl acrylate (EA), *N,N*-dimethyl formamide (DMF), iron(II) sulfate heptahydrate ($FeSO_4 \cdot 7H_2O$). Deionized water (DW) with 18 MΩ cm resistivity was used. The Cd^{2+}, Pb^{2+} and As(V) stock solutions were prepared with DW using $Na_2HAsO_4 \cdot 7H_2O$ (Sigma–Aldrich), cadmium nitrate (J.T. Baker, reagent grade) and lead nitrate (J.T. Baker, reagent grade), respectively, and diluted prior to use. Adjustment of pH was accomplished with 0.1 M NaOH and 0.1 M HNO_3 (Sigma Aldrich). Concentrations of arsenic species were given as elemental arsenic concentration. Coupling agent *N,N*-diisopropylethylamine and HNO_3 ultrapure were supplied (Fluka), sodium hydroxide (NaOH), methanol for UV-spectroscopy, ≥99.8%, (Sigma Aldrich) were used as obtained.

Adsorbents preparation

A1/ and A2/MWCNT adsorbents were obtained by the modification of hydrophobic MWCNT surface by performing successive amidation/nucleophilic addition reactions, which provide the introduction of amino terminated branched structure on adsorbents surface. This approach allows the introduction of the number of amino functional groups in successive steps. Oxidation and amino functionalization multilayer carbon nanotubes is performed with ethylenediamine according to the procedure described previously.[16] Obtained e-MWCNT was further functionalized with controlled successive introduction of ethyl acrylate and EDA in a multi-step procedure (Scheme S-1 in the Supplementary material to this paper).

Syntheses of amino modified MWCNT

Ethyl acrylate (50 mL) and *N,N*-diisopropylethylamine (50 mL) were added to a suspension of e-MWCNT (1.0 g) in dry methanol (100 mL), and the resulting mixture was stirred at 80 °C for 3 days. The obtained mixture was then filtered on a Millipore membrane (PTFE, 0.22 μm), and the solid on the filter was washed with CH_2Cl_2 and diethyl ether. The nanotubes were then allowed to react with EDA (100 mL) in methanol (100 mL) at 80 °C for 3 days to give first-generation grafted MWCNT, *i.e.*, A1/MWCNT. In an analogous way, starting from A1/MWCNT (Scheme S-1, c), was synthesized the second generation of amino terminal adsorbent, *i.e.*, A2/MWCNT material (Scheme S-1, e).

Synthesis of A1/MWCNT–α-FeO(OH) and A2/MWCNT–α-FeO(OH)

A1/ and A2/MWCNT (1 g) was sonicated in DW (50 mL) with simultaneous introduction of N_2 for 30 min. The reaction was continued, under magnetic stirring and inert atmosphere, by the drop-wise addition 13 mL of $FeSO_4 \cdot 7H_2O$ solution (0.18 mol L^{-1}) for 15 min. Ferri/ferro oxidation was performed by changing nitrogen flow with air, and neutralizing the reaction mixture with 6 mL of 0.25 mol L^{-1} $NaHCO_3$ solution to cause precipitation of iron-

(CC) 2017 SCS.

(oxy)hydroxide in goethite form.[15,17] Reaction took place for 48 h while green–blue color of solution changed to ochre shade. Obtained product was filtered, washed with DW, and freeze/ /dried was conducted by cooling and keeping freshly obtained material at –30 °C for 24 h, followed by freeze drying at –50 °C maintaining 0.05 mbar for 24 h, and process was finished at –70 °C and 0.01 mbar for 1 h. Obtained adsorbents were denoted as A1/ and A2/ /MWCNT–*α*-FeO(OH).

Details of adsorption experiments and adsorbent characterization are described in the Supplementary material to this paper.

RESULTS AND DISCUSSION

Optimization of adsorbents syntheses

Optimization of A1/ and A2/MWCNT adsorbents syntheses, and subsequent iron(oxy)hydroxide loading on former materials to produce A1/ and A2/ /MWCNT–*α*-FeO(OH) high performance adsorbents were performed. The optimization goals were defined in relation to: adsorption efficiency (capacity/reusability) and adsorption kinetic. The optimization of adsorbent preparation was performed according to the previously published methodology;[18] selection of optimal pH value 6,0 and initial concentration of 5 ppm for all analysed pollutants, were established accordingly.

Obtained results for adsorption capacities are given in Table I. The maximum adsorption capacities of A1/ and A2/MWCNT adsorbents with respect to Cd^{2+} and Pb^{2+} indicate that higher number of amino groups contribute to greater adsorption capacities. Low increase of adsorption capacity of A2/MWCNT–*α*-FeO(OH), in comparison to A1/MWCNT–*α*-FeO(OH), with respect to As(V) was obtained. Additionally, higher number of amino groups in A2/MWCNT also contributed to effective iron loading, and thus higher adsorption capacity of As(V) was obtained for A2/MWCNT–*α*-FeO(OH).

TABLE I. Adsorption capacities of all studied adsorbents and amino group content of A1/ and A2/MWCNT adsorbents

Adsorbent	q_m/mg g^{-1} (Langmuir model)			Amino group content, mmol g^{-1}
	Cd^{2+}	Pb^{2+}	As(V)	
A1/MWCNT	31.31	45.92	15.6	1.38
A2/MWCNT	44.18	60.12	18.8	1.87
A1/MWCNT-*α*-FeO(OH)	–		25.2	–
A2/MWCNT-*α*-FeO(OH)	–		27.6	–

The increased number of total basic sites on A1/ and A2/MWCNT adsorbents contributed to the increased adsorption capacity toward Cd^{2+} and Pb^{2+}, and lowered with respect to As(V). The significance of the amino group involved in the cation complexation was recently unequivocally proved.[19] According to calculated theoretical stoichiometric ratio of carboxyl[14] with respect to the introduced polyamidoamino functionalities it could be expected 1.74 and 3.48 mmol

(CC) 2017 SCS.

g^{-1} of total basic sites in A1/ and A2/MWCNT adsorbents, respectively. Somewhat lower experimental values of 1.38 and 1.87 mmol g^{-1} (Table I) indicated that the extent of functionalization was lower due to increased surface crowdedness which caused decreased efficiency of any subsequent reaction steps. Additionally, the methodology applied for synthesis of A1/ and A2/MWCNT–*α*--FeO(OH) provided the means for controlled precipitation of hydrous iron oxide in the goethite form with a number of available adsorptive sites effective for As(V) removal.[9,10,12,18] No significant increase of the adsorption capacity of these adsorbents, comparing to A1/ and A2/MWCNT precursor materials, was obtained. Considering the simplicity of A1/MWCNT adsorbent synthesis and adsorption capacity of A1/MWCNT–*α*-FeO(OH) *vs.* A2/MWCNT–*α*-FeO(OH) only former materials were further used in adsorption experiment.

Textural properties and pH_{PZC}

The physical properties of studied adsorbents are presented in Table II. The specific surface area, pore volume and average pore diameter were determined from adsorption/desorption isotherms.

Amino groups on A1/ and A2/MWCNT show basic properties thus pH_{PZC} were found to be 5.76 and 5.92, respectively. According to the electrostatic interactions, adsorption of Cd^{2+} and Pb^{2+} on A1/ and A2/MWCNT adsorbents is favoured at higher pH values than pH_{PZC}, due to the more negative charged adsorbents surface.

TABLE II. Textural properties and pH_{PZC} of studied adsorbents

Adsorbent	Specific surface area $m^2\ g^{-1}$	Pore volume $cm^3\ g^{-1}$	Average pore diameter, nm	pH_{PZC}
A1/MWCNT	98.54	0.554	20.1	5.76
A2/MWCNT	99.66	0.584	21.0	5.92
A1/MWCNT–α-FeO(OH)	115.82	0.242	18.8	6.96
A2/MWCNT–α-FeO(OH)	119.44	0.292	19.7	7.12

Similar phenomena stand for A1/ and A2/MWCNT–*α*-FeO(OH) adsorbents, where an increasing negative surface potential at pH values higher than pH_{PZC} (6.96 and 7.12 for A1/ and A2/MWCNT–*α*-FeO(OH), respectively) is due to the deprotonation of hydroxyl groups present on the adsorbent surface.[9,12,10] Improved textural parameters of A1/ and A2/MWCNT–*α*-FeO(OH), *i.e.*, increased specific surface area, indicates higher availability of surface active sites for interactions with arsenic species.

FTIR characterization

FTIR spectra of A2/MWCNT and A1/MWCNT–*α*-FeO(OH) before and after metal ions adsorption are shown in Fig. 1. FTIR spectra of A2/MWCNT

(CC) 2017 SCS.

before adsorption shows high intensity peak at 3351 cm^{-1} that corresponds to the stretching vibrations of amino group, and the lower intensity peak at 3528 cm^{-1} corresponding to the stretching vibrations of OH group. Strong peak at 2938 cm^{-1} relates to the stretching vibrations of methylene group.

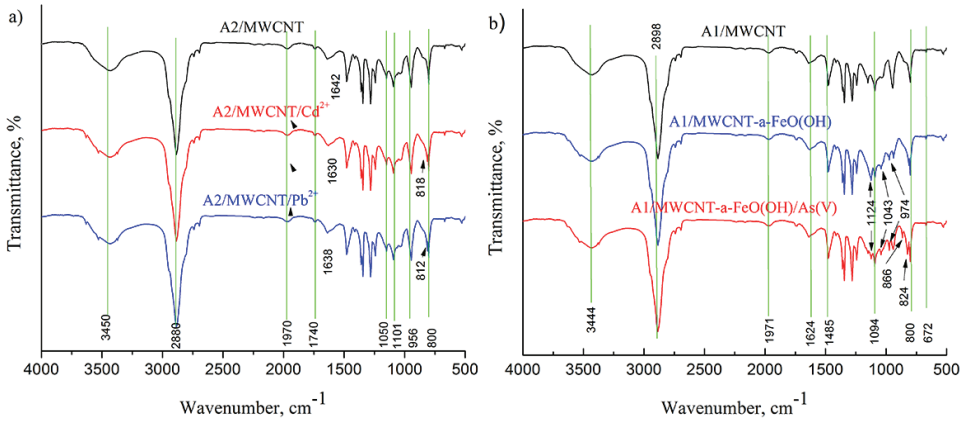

Fig. 1. FTIR spectra of A2/MWCNT before and after the adsorption of Cd^{2+} and Pb^{2+} (a) and FTIR spectra of A1/MWCNT and A1/MWCNT–α-FeO(OH) before and after adsorption of As(V) (b); C_i = 5 mg L^{-1}, m/V = 100 mg L^{-1}, pH 6.0).

The FTIR transmission spectrum of A2/MWCNT shows a low intensity band at ≈1740 cm^{-1}, and a band observed at lower frequency, ≈1640 cm^{-1}, assigned to stretching of the amide carbonyl (C=O) group. In addition, the presence of new bands at ≈1580 and ≈1180 cm^{-1}, correspond to N–H in-plane and C–N bond stretching, respectively. A band at ≈800 cm^{-1} is due to the out-of--plane NH_2 bending mode.

FTIR spectra of the metallic complexes (A2/MWCNT/Cd^{2+}, A2/MWCNT/ /Pb^{2+} and A1/MWCNT–α-FeO(OH))/As(V)), Fig. 1, were recorded on the samples obtained after metal adsorption on A2/MWCNT and A1/MWCNT– –α-FeO(OH), respectively, using different initial concentration of a pollutant. Adsorption bands shifts and peak intensities increase or decrease corresponding to the newly created adsorbent-metallic complexes that include C=O, CH, NH, CN and C=N groups (Table S-I in the Supplementary material). Minor shifts can be noticed at lower wavelengths for CO, C=N, CN and CH groups due to stretching vibrations of bands from functionalized nanomaterials as it is shown in Table S-I. If compared, FTIR spectra of A2/MWCNT and A1/MWCNT–α-FeO(OH) and metal complex with A2/MWCNT and A1/MWCNT–α-FeO(OH) show the increasing of bond lengths after the formation of metal complexes. Due to lack of electrons in nitrogen, the vibration of NH group peak shifts towards the higher wavelength.[9,15,18]

(CC) 2017 SCS.

On the other side, the peaks assigned to the Fe–OH bands, present on A1/ /MWCNT–α-FeO(OH) surface, appeared at 1124, 1043 and 974 cm^{-1} (Table S-I). These peaks almost disappear in the spectra of A1/MWCNT–α-FeO(OH)/As(V) at As(V) concentration >3 ppm. On the other hand, the new bands, which correspond to As–O stretching vibration of coordinated arsenic species, appeared at 824 and 866 cm^{-1}.[20] The stretching vibration of the band which corresponds to complexed As–O–Fe was found at lower frequency, 828 cm^{-1}, while wavelength of the uncomplexed/unprotonated As–O–Fe is located at higher value, 866 cm^{-1}. The shorter bond length results in a stronger force constant, and it is reflected as higher infrared frequency.[9] At higher surface coverage bidentate binuclear complex is a preferential type of arsenic binding.[21]

Effect of pH on adsorption process

Adsorption efficiency of As(V), Cd^{2+} and Pb^{2+} on the adsorbent was studied at pH range between 3.0 and 10 (Fig. 2). The pH value of the solution influences the surface charge of the adsorbent, the degree of ionization, the content of the metal species in the aqueous solutions and the surface properties of the adsorbent. It is known that the speciation of heavy metals in the water depend on the pH value, and different forms could exist: Cd^{2+}, $Cd(OH)^{+}$ and $Cd(OH)_{2(s)}$ (Fig. 2a),[14] Pb^{2+}, $Pb(OH)^{+}$ and $Pb(OH)_{2(s)}$ (Fig. 2b),[6,17] and arsenic in the form of H_3AsO_4, $H_2AsO_4^{-}$, $HAsO_4^{2-}$, AsO_4^{3-} species (Fig. 2c).[12] At pH values lower than 9.0 the dominant type of Cd^{2+} is present in the form of the $[Cd(H_2O)_6]^{2+}$.[14]

It can be seen that A2/MWCNT shows the best sorption capacity for the adsorption of Cd^{2+} in the pH interval 5.0–8.0. Amino groups on A2/MWCNT, acids having a pK_a value greater than 7.0 [10,14] and pH_{PZC} 5.92, contribute mostly to the adsorption of Cd^{2+}.

Decrease of the adsorption capacity for A2/MWCNT by Cd^{2+}, at pH values higher than 9.0, coincides with the decreasing concentration of Cd^{2+} and an increase in the concentration of ionic species which have a lower affinity for the amino groups. The precipitation of $Cd(OH)_2$, at pH > 9.0, is dominant process. The precipitated $Cd(OH)_2$, at pH values higher than 9.0, occupies adsorption places on the adsorbent, preventing the adsorption of Cd^{2+} with increasing pH.

Apparently, removal of Cd^{2+} at pH ≥ 9.0 is a combination of the two effects, the precipitation of $Cd(OH)_2$, and the adsorption onto the adsorbent. Based on these results, the pH value of 6.0 was selected as optimal value for Cd^{2+} removal. Similar behaviour was found for Pb^{2+} and optimal pH value 6.0 for lead adsorption was also selected.

The adsorption of As(V) ions on the adsorbent A1/MWCNT–α-FeO(OH) is more favourable at pH values lower than 7.12 pH_{PZC}. At $pH_i < pH_{PZC}$ the As(V) removal percentages was in the range from 91.0 to 97.0 %. The electrostatic interaction between the positively charged surface of the adsorbent and the negatively

(CC) 2017 SCS.

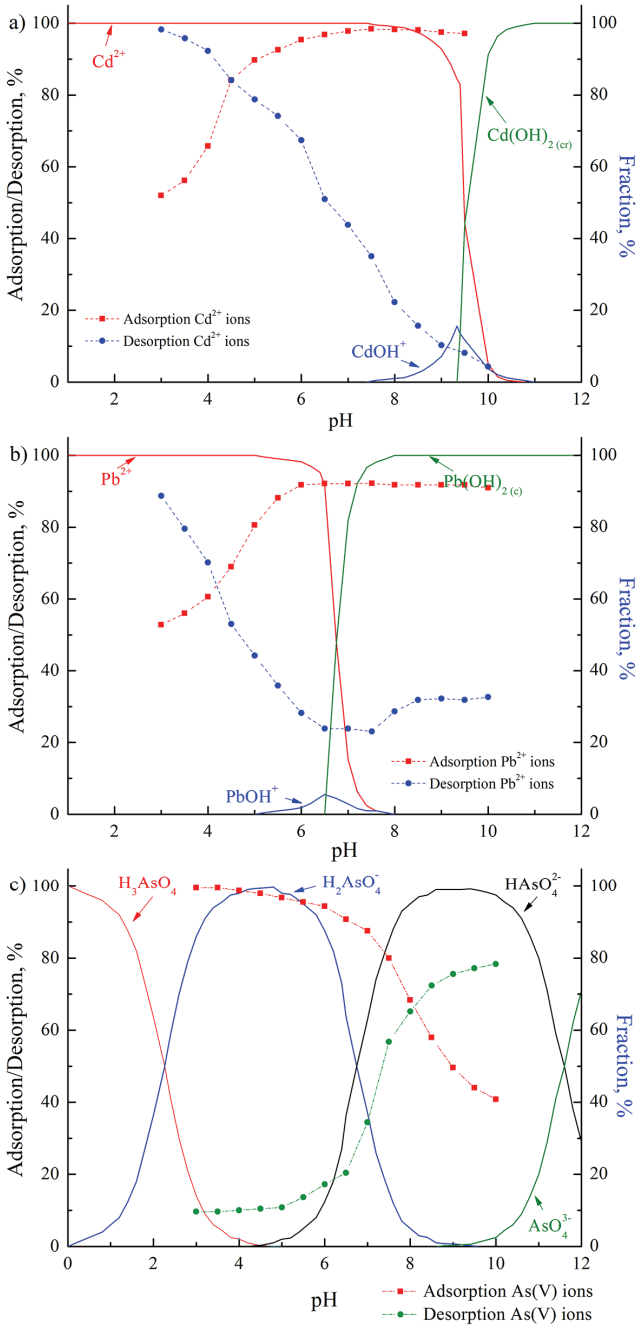

Fig. 2. The effect of pH on the formation of ionic species adsorption and desorption of Cd^{2+} (a), Pb^{2+} on A2/MWCNT (b), and As(V) at A1/MWCNT-α-FeO(OH) (c); C_i = 0.2 mg L^{-1}, m/V = 100 mg L^{-1}, t = 90 min, T = 298 K.

(CC) 2017 SCS.

charged ionic species of arsenic, monovalent anion $H_2AsO_4^-$ (pKa_1 2.3), leads to more favorable adsorption. Main factor contributing to lower adsorption of arsenic at $pH_i > pH_{PZC}$ is surface group ionization of iron(III) oxide hydroxyl groups that develop negative charge at adsorbent surface. At higher pH the presence of divalent As(V) anion dominates in solution and repulsion with negative adsorbent surface cause lower adsorption efficiency. The pH change during adsorption is an indication that protonation/deprotonation reactions of surface functional group together with adsorption of arsenic species are operative.

An important property of adsorbent is the ability for reusing after the regeneration process. Such an adsorbent, not only should possess a high adsorption capacity, but also good desorption properties, which significantly reduces the total cost of the adsorbent. Desorption percentages of Cd^{2+}, Pb^{2+} and As(V), and ions in solutions at different pH values are also shown in Fig. 2. Desorption of Cd^{2+}increases with the decrease in pH. About 45 % of Cd^{2+} is desorbed at pH 7.0. The sudden desorption increase occurs at pH < 7 and reaches a value of 99 % at pH 2.0 (Fig. 2a). Desorption of As(V) is reduced as pH decrease. About 30 % of As(V) is desorbed at pH 6.5. The sudden desorption increase occurs at pH > 6.5, and reaches a value of 78 % at pH 10 (Fig. 2b). Incomplete desorption indicates that part of the arsenic is permanently chemically bound to the adsorbent.

Adsorption isotherms

The earliest-known relationships that describe the adsorption are Freundlich and Langmuir isotherms.[22] Langmuir isotherm implies the formation of monolayer on a energetically homogeneous surface, while Freundlich isotherm implies the existence of heterogeneous surfaces with uneven distribution of adsorption sites with different heat of adsorption and the possibility to create multilayer adsorption.[18] These isotherms, as well as Dubinin–Radushkevich and Temkin isotherm models were used to correlate different isotherms to the experimental data[10,23]; our results showed better fit for the adsorption of Cd^{2+}, Pb^{2+} and As(V) ions at 298, 308 and 318 K with Langmuir and Freundlich isotherm, shown in Fig. 3.

Langmuir (Fig. 3a) and Freundlich (Fig. 3b and c) parameters are presented in Table III; Dubinin–Radushkevich and Temkin parameters are given in Table S-II in the Supplementary material. It can be noticed that for the adsorption of Cd^{2+} the r values for Langmuir model is larger, and that Δq values and calculated standard errors of parameters are lower than for the Freundlich model. This results indicates that the Langmuir model better describes Cd^{2+} adsorption. While the adsorption of Pb^{2+} and As(V) ions shows that r has higher value and that Δq and calculated standard errors of parameters have lower values which indicates that Freundlich model better describes the adsorption of these ions. For all three ions adsorption on selected adsorbents, q_{max} and b values increase with increasing

(CC) 2017 SCS.

temperature; the adsorption capacity for these ions is greater at higher temperatures, while standard errors of these parameters very little deviate. It is clear that highest adsorption capacity for these ions is achieved at elevated temperature.

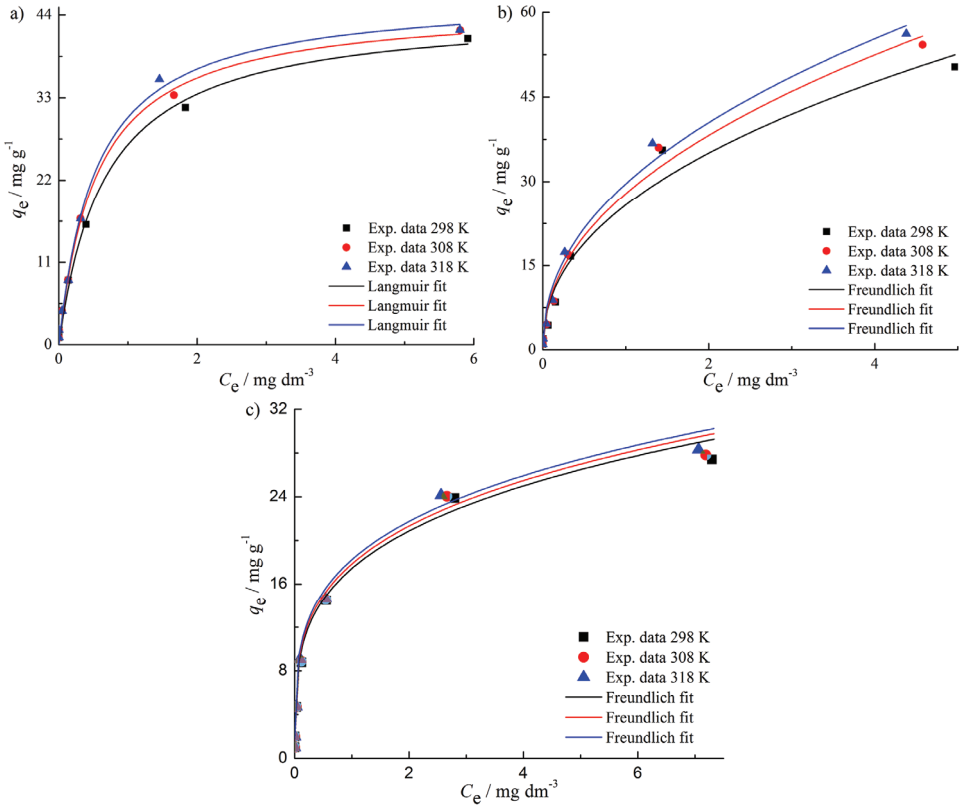

Fig. 3. The adsorption isotherms of Cd^{2+} (a) and Pb^{2+} (b) on A2/MWCNT, and As(V) ion on A1/MWCNT–α-FeO(OH) (c) at 298, 308 and 318 K (m/V = 100 mg L^{-1} and pH 6.0).

The essential features of the Langmuir isotherm may be expressed in terms of the dimensionless separation factor, K_R, given by Eq. (1), which define whether an adsorption process is favourable or not:

$$K_R = \frac{1}{1 + bC_0} \tag{1}$$

where C_0 is initial concentration (mg L^{-1}) and b is Langmuir constant (L mg^{-1}) obtained from adsorption isotherm. The K_R value implies the quality of adsorption: $K_R > 1$ indicates that adsorption is unfavourable, $K_R = 1$ means linear adsorption, favourable case gives $0 < K_R < 1$ and irreversible $K_R = 0$.[18,24]

Values of K_R, in the range 0.0199–0.699 for Cd^{2+}, 0.042–0.84 for Pb^{2+} and 0.011–0.55 for As(V), indicate favourable adsorption of these ions.

(CC) 2017 SCS.

TABLE III. Adsorption isotherm parameters for As(V) on A1/MWCNT–α-FeO(OH), and Pb^{2+} and Cd^{2+} on A2/MWCNT

Isotherm model	Cd^{2+}			Pb^{2+}			As(V)		
	T / K								
	298	308	318	298	308	318	298	308	318
Langmuir									
q_m / mg g^{-1}	42.75	43.91	44.18	54.72	58.43	60.12	27.21	27.47	27.55
K_L /L mg^{-1}	2.649	2.958	3.069	1.88	2.03	2.26	4.291	4.641	4.918
Δq / %	3.32	2.66	3.11	3.98	4.09	3.87	2.98	2.79	3.06
R^2	0.987	0.990	0.991	0.97	0.963	0.965	0.991	0.989	0.990
Freundlich									
K_F / mg g^{-1} $(dm^3\ mg^{-1})^{1/n}$	21.299	22.724	23.207	23.502	25.760	27.549	15.817	16.198	16.520
$1/n$	0.455	0.457	0.457	0.454	0.457	0.456	0.343	0.344	0.342
Δq / %	4.13	4.21	4.12	3.56	3.98	3.45	2.12	2.57	3.01
R^2	0.976	0.973	0.977	0.970	0.979	0.981	0.993	0.991	0.993

Thermodynamic consideration

Adsorption data obtained on different temperature were used for calculation of Gibbs energy (ΔG^0), enthalpy (ΔH^0) and entropy (ΔS^0) changes using the Van't Hoff thermodynamic equations, Eqs. (2) and (3):[1,9,18,25]

$$\Delta G^0 = -RT \ln b \tag{2}$$

$$\ln b = \frac{\Delta S^0}{R} - \frac{\Delta H^0}{(RT)} \tag{3}$$

Langmuir constant b is obtained from isothermal experiments (Table III), while ΔH^0 and ΔS^0 are calculated from the slope and intercept of the linear function $\ln b$–T^{-1}, assuming that the kinetics of adsorption takes place in stationary conditions.

The calculated thermodynamic values (Table IV) can provide some information on the mechanisms of adsorption on synthesized adsorbents.

TABLE IV. Calculated Gibbs energy, enthalpy and entropy changes for Cd^{2+}, Pb^{2+} and As(V) adsorption

Adsorbent	Ion	ΔG^0 / kJ mol^{-1}			ΔH^0	ΔS^0
		298 K	308 K	318 K	kJ mol^{-1}	J mol^{-1} K^{-1}
A2/MWCNT	Cd^{2+}	–41.20	–42.86	–44.35	5.83	157.82
A2/MWCNT	Pb^{2+}	–54.31	–56.39	–58.57	9.23	213.05
A1/MWCNT–α-FeO(OH)	As(V)	–41.39	–42.98	–44.53	5.38	156.90

The negative ΔG^0 values indicate that the adsorption of As(V), Cd^{2+} and Pb^{2+} are spontaneous processes. Obtained ΔG^0 values, being between –20 and –80 kJ mol^{-1} implies that the interaction between the adsorbent and Cd^{2+}, Pb^{2+} and

(CC) 2017 SCS.

As(V) is the result of contributions of physical sorption and chemisorption processes.[9,18]

Indication that ΔG^0 decreased with the increasing temperature means higher adsorption efficiency at higher temperature. The lowest ΔG^0 value was obtained for Cd^{2+} adsorption on A2/MWCNT at 318 K as a consequence of its higher mobility. Regardless of the coordinating solvents, at higher temperatures, solvated Cd^{2+} are easily desolvated, and diffusion through the boundary layer and within the pores is a faster process.

The positive ΔH^0 values indicate that the adsorptions of Cd^{2+}, $Pb^{2+}$and As(V) are endothermic processes. A possible explanation of endothermic nature is that an ion, for example $[Cd(H_2O)_6]^{2+}$, solvated in water needs energy to desolvate, to make it available to interact with the surface of the adsorbent. Removing the water molecules from $[Cd(H_2O)_6]^{2+}$ is an endothermic process, and based on the total value ΔH^0 of the adsorption process, it can be concluded that the process of desolvation significantly exceeds the adsorption enthalpy change.

It is generally recognized that the physical adsorption includes enthalpy change between 2 and 21 kJ mol^{-1}, while enthalpy change of chemisorption is in the range of 80–200 kJ mol^{-1}.[9] From this point of view, one could conclude that in the adsorption of As(V), Cd^{2+} and Pb^{2+} the physisorption mechanism dominates.

The positive values of entropy change (ΔS^0) indicate the increasing of the disorder at the interface solid-liquid, *i.e.*, between the adsorbate and the adsorbent from the solution, during the process of adsorption. The adsorbate binding causes a reduction in the degree of freedom of the system. In some processes, such as ion exchange, surface ions are released into solution, thus increasing the overall entropy of the system.[19]

Adsorption kinetics

Removal of Cd^{2+}, Pb^{2+} and As(V) ions from aqueous solution, as a function of the contact time is shown in Fig. 4. Adsorption on all three adsorbents, shows rapid increase with the increase of the contact time, and after 90 min adsorption equilibrium was established. This contact time was used in the subsequent adsorption experiments. A large number of kinetic adsorption models: pseudo-first, pseudo-second order, Elovich and intra-particular Weber–Morris model (W–M) are used for modelling of kinetic data.[13,26] According to the regression coefficient and calculated standard error parameters for all four models, the experimentally obtained kinetic data are best described by the pseudo-second order kinetics (Eq. (4)):

$$\frac{t}{q_t} = \frac{1}{K' q_e^2} + \frac{1}{q_e} t \qquad (4)$$

(CC) 2017 SCS.

where q_e and q_t, mg g^{-1}, are amount of adsorbed ions at adsorption equilibrium and in time t, respectively, while K', g mg^{-1} min^{-1}, is rate constant for pseudo-second order adsorption kinetics.

The values of q_e, K', r and Δq are given in Table V.

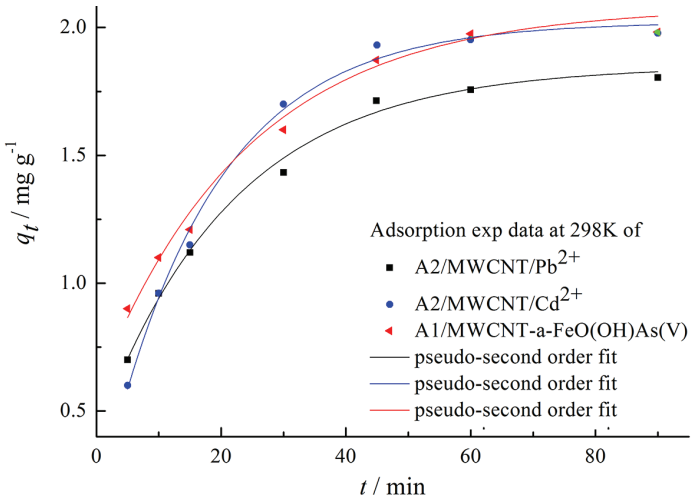

Fig. 4. Time dependent adsorption of Pb^{2+} and Cd^{2+} on A2/MWCNT, and As(V) ion on A1/MWCNT–α-FeO(OH) ($C_{i[Pb^{2+}]}$ = 0.5 mg L^{-1}, $C_{i[Cd^{2+}]}$ = 0.2 mg L^{-1}, $C_{i[As(V)]}$ = 0.2 mg L^{-1}, m/V = 100 mg L^{-1}, T = 298 K, pH 6.0).

TABLE V. The parameters of the kinetic model of pseudo-second order for the adsorption of Pb^{2+} and Cd^{2+} on A2/MWCNT, and As(V) ions on A1/MWCNT-α-FeO(OH) ($C_{i[Pb^{2+}]}$ = 0.5 mg L^{-1}, $C_{i[Cd^{2+}]}$ = 0.2 mg L^{-1}, $C_{i[As(V)]}$ = 0.2 mg L^{-1}, m/V = 100 mg L^{-1}, T = 298 K, pH 6.0)

Ion	q_e / mg g^{-1}	K' / g mg^{-1} min^{-1}	Δq / %	r
Cd^{2+}	2.338±0.21	0.0329±0.0007	2.07	0.993
Pb^{2+}	2.042±0.18	0.0452±0.0012	2.78	0.996
As(V)	2.234±0.04	0.0446±0.0010	2.21	0.993

Considering the values of constants K', it can be concluded that the fastest adsorption equilibrium was achieved in the case of adsorption of Cd^{2+} on A2/MWCNT. Slower reaching equilibrium occurs with Pb^{2+} and As(V) showing that the two processes have higher energy barrier,[10,15] like chemisorption and/or surface complexation. The confirmation of the pseudo-second order kinetics, which is common for the removal of the metal ions, means that the concentration of the adsorbate Cd^{2+} and Pb^{2+}on A2/MWCNT, and As(V) on A1/MWCNT–α--FeO(OH) adsorbent surface sites are involved in the step that determines the rate of adsorption process.[10,14,17]

In order to define the rate determining step of the overall adsorption process the W–M model was used. This model include four consecutive steps: mass

(CC) 2017 SCS.

transport in the bulk, diffusion through the liquid film surrounding the surface of the particle (film diffusion), diffusion through the pores inside of particles (intra-particle diffusion) and adsorption/desorption of adsorbate with active sites at adsorbent surface (*i.e.*, participation of the mass transfer in the overall adsorption process). Results are given in Table VI and Fig. 5.

TABLE VI. The rate constants of intra-particle diffusion kinetic modelling

Step	Constant	A2/MWCNT/Cd^{2+}	A2/MWCNT/Pb^{2+}	A1/MWCNT–α-FeO(OH)/As(V)
Step 1 (Intra-particle diffusion)	k_{p1} / mg g^{-1} $min^{-0.5}$	0.3349	0.2231	0.2145
	C / mg g^{-1}	–0.1325	0.2305	0.4115
	R^2	0.996	0.986	0.995
Step 2 (Equilibrium)	k_{p2} / mg g^{-1} $min^{-0.5}$	0.0167	0.0206	0.0043
	C / mg g^{-1}	1.8203	1.9414	1.9414
	R^2	0.993	0.992	0.995

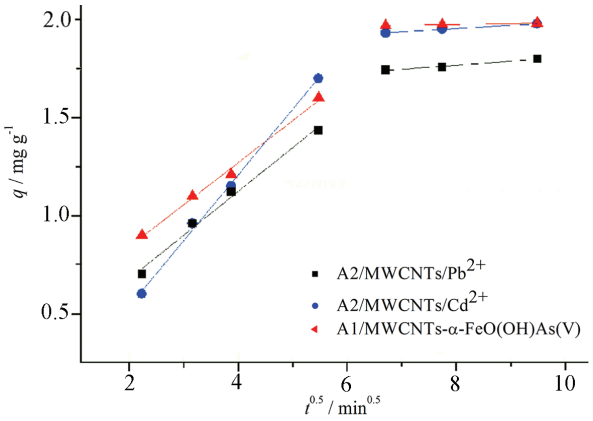

Fig. 5. Intra-particle diffusion plots at 298 K ($C_{i[Pb^{2+}]}$ = 0.5 mg L^{-1}, $C_{i[Cd^{2+}]}$ = 0.2 mg L^{-1}, $C_{i[As(V)]}$ = 0.2 mg L^{-1}, m/V = 100 mg L^{-1}, T = 298 K, pH 6).

The W–M fitting revealed that two successive linear steps (Fig. 5) could describe adsorption process: fast kinetics in the first step followed by very slow attainment of equilibrium in second part. A larger intercept found for the A1/ /MWCNT–α-FeO(OH)/As(V) system indicates higher resistance, *i.e.*, slower ionic transport due to intra-particle diffusion. The first linear part describe external mass transfer from bulk solution to the most available adsorptive surface, while the second part represent processes of high dependence on adsorbent porosity, *i.e.*, pore geometry and network density. Due to the concentration gradient the ions diffuse through bulk solution and tree-like porous system which extend into adsorbent interior approaching to all available surface active sites. The intra-particle and film diffusion resistance slow down the adsorbate transport, *i.e.*, net

(CC) 2017 SCS.

transport in a direction of variable time-dependent concentration gradient. At the final stage of process, the adsorption takes place at low rate until saturation of all available surface sites is achieved.[9,18]

Activation energy

Known Arrhenius type dependence of rate constant on temperature, Eq. (5):

$$\ln K' = -\frac{E_a}{RT} + \ln A \tag{5}$$

can help in understanding of the mechanism of the metal ion adsorption.

Calculated activation energies (kJ mol^{-1}) in studied adsorption are as follows: 8.846 for Cd^{2+}, 9.25 for Pb^{2+} and 7.98 for As(V). Relatively close values of activation energies for Cd^{2+} and Pb^{2+} adsorption indicate that the adsorption mechanism for both cations involves similar activated complex depending on the Van der Waals radius of the cation considered. The fact that physisorption generally has the activation energy bellow 40 kJ mol^{-1} and chemisorption above 40 kJ mol^{-1},[14,15] indicates that both types of adsorption processes take place by the formation of mainly non-covalent interactions. In practice, both physisorption and chemisorption can be expected to be operative in the course of adsorption process which means that formation of one chemisorbed layer could be covered by a physically adsorbed pollutant forming a multilayered structure of adsorbed pollutants.[14,15]

CONCLUSIONS

In this work, MWCNT modified with polyamidoamine dendrimers produced an efficient adsorbents A1/ and A2/MWCNT capable for Cd^{2+}, Pb^{2+} and As(V) removal from natural water. The increased numbers of amino terminal functionalities of A2/MWCNT material contributed to better adsorption performance than A1/MWCNT. Furthermore, the controllable precipitation of α-FeOOH on A1/ and A2/MWCNT produced novel A1/ and A2/MWCNT–α-FeO(OH) adsorbents, respectively, useful for As(V) removal. Due to the complexcity of A2/MWCNT synthesis and low increases of adsorption potential of A2/MWCNT–α-FeO(OH) with respect A1/MWCNT–α-FeO(OH), larger usefulness of former one for As(V) removal is indicated. The adsorption data were modelled by using Langmuir and Freundlich isotherm, while kinetic data was successfully fitted by using pseudo-second-order equation and Weber–Morris model. Desorption experiments indicated a good recovery and repeated use after performing five desorption adsorption/desorption cycles. Thermodynamic parameters revealed that the adsorption processes were favourable and more spontaneous at higher temperature. Results showed that studied adsorbents are efficient and reusable for Cd^{2+}, Pb^{2+} and As(V) removal from natural water.

(CC) 2017 SCS.

SUPPLEMENTARY MATERIAL

Details of adsorption experiments, adsorbent characterization, Dubinin–Radushkevich and Temkin adsorption isotherms parameters and comments on surface complex formation and competitive adsorption are available electronically at the pages of the journal website: http://www.shd.org.rs/JSCS/, or from the corresponding author on request.

Acknowledgements. The authors acknowledge the financial support from the Ministry of Education, Science and Technological Development of the Republic of Serbia, grant numbers III45019, OI 172057, OI 172013 and the University of Defense, grant number VA-TT/4-16--18.

И З В О Д

УКЛАЊАЊЕ ТЕШКИХ МЕТАЛА ИЗ ВОДЕ КОРИШЋЕЊЕМ ВИШЕСТЕПЕНО ФУНКЦИОНАЛИЗОВАНИХ ВИШЕСЛОЈНИХ УГЉЕНИЧНИХ НАНОЦЕВИ

ДРАГОСЛАВ БУДИМИРОВИЋ[1], ЗЛАТЕ С. ВЕЛИЧКОВИЋ[2], ЗОРАН БАЈИЋ[2], ДРАГАНА Л. МИЛОШЕВИЋ[3], ЈАСМИНА Б. НИКОЛИЋ[1,*], САША Ж. ДРМАНИЋ[1] и АЛЕКСАНДАР Д. МАРИНКОВИЋ[1]

[1]*Универзитет у Београду, Технолошко–металуршки факултет, Карнегијева 4, 11120 Београд,* [2]*Универзитет одбране, Војна академија, Павла Јуришића-Штурма 33, Београд и* [3]*Институт за хемију, технологију и металургију, Универзитет у Београду, Његошева 12, Београд*

У оквиру овог рада проучавана је синтеза и карактеризација вишеслојних угљеничних наноцеви (MWCNT) модификованих дендримерима полиамидоамина, A1/ /MWCNT и A2/MWCNT, коришћених за уклањање катјона. Овим приступом је омогућено сукцесивно увођење амино група. Такође, адсорбенти на бази A2/MWCNT и гетита α-FeOOH, A2/MWCNT–α-FeO(OH), су коришћени за уклањање As(V) јона. Утицај pH, времена контакта, почетних концентрација јона и температуре на ефикасност адсорпције је испитивана у шаржним системима. Одређивањем адсорпционих капацитета, коришћењем Лангмировог (Langmuir) модела, добијена је вредност од 18,8 mg g^{-1} за As(V), 60,1 и 44,2 mg g^{-1} за Pb^{2+} и Cd^{2+} на A2/MWCNT, редом. Такође, добијене су вредности од 27,6 и 29,8 mg g^{-1} за уклањање As(V) на A1/ и A2/MWCNT–α-FeO(OH), редом. Термодинамички параметри су показали да је адсорпција спонтан и ендотерман процес. Резултати испитивања утицаја конкурентних јона: бикарбоната, сулфата, фосфата, силиката, хромата, флуорида и природних органских материја (NOM), тј. хуминске киселине (HA), су указали на највећи утицај фосфата на смањење адсорпције арсената. Временски зависна адсорпција је најбоље описана кинетичким моделом псеудо-другог реда и Вебер–Морисовим (Weber–Morris) моделом међучестичне дифузије која је одредила укупну брзину сорпционог процеса. Поред овога, енергија активације (E_a / kJ mol^{-1}), је израчуната из кинетичких података и износила је: 8,85 за Cd^{2+}, 9,25 за Pb^{2+} и 7,98 за As(V).

(Примљено 22. априла, ревидирано 29. маја, прихваћено 29. маја 2017)

REFERENCES

1. Z. J. Bajić, Z. S. Veličković, V. R. Djokić, A. A. Perić-Grujić, O. Ersen, P. S. Uskoković, A. D. Marinković, *Clean – Soil, Air, Water* **44** (2016) 1
2. S. Lata, and S. R. Samadder, *J. Environ. Manage.* **166** (2016) 387
3. N. V. Ihsanullah, F. A. Al-Khaldi, B. Abusharkh, M. Khaled, M. A. Atieh, M. S. Nasser, T. Laoui, T. A. Saleh, S. Agarwal, I. Tyagi, V. K. Gupta, *J. Mol. Liq.* **204** (2015) 255
4. M. R. Lasheen, I. Y. El-Sherif, D. Y. Sabry, S. T. El-Wakeel, M. F. El-Shahat, *Desalin. Water Treat.* **53** (2015) 3521

(CC) 2017 SCS.

5. N. Ünlü, and M. Ersoz, *J. Hazard. Mater.* **136** (2006) 272
6. L. Gao, H. Yin, X. Mao, H. Zhu, W. Xiao, D. Wang, *Environ. Sci. Pollut. Res.* **22** (2015) 14201
7. S. Lazarević, I. Janković-Častvan, B. Jokić, Đ. Janaćković, R. Petrović, *J. Serb. Chem. Soc.* **81** (2016) 197
8. N. V. Ihsanullah, A. Abbas, A. M. Al-Amer, T. Laoui, M. J. Al-Marri, M. S. Nasser, M. Khraisheh, M. A. Atieh, *Sep. Purif. Technol.* **157** (2016) 141
9. Z. Veličković, G. D. Vuković, A. D. Marinković, M. S. Moldovan, A. A. Perić-Grujić, P. S. Uskoković, M. D. Ristić, *Chem. Eng. J.* **181**–**182** (2012) 174
10. Z. Veličković, Z. Bajić, M. Ristić, V. Đokić, A. Marinković, P. Uskoković, M. Vuruna, *Dig. J. Nanomat. Biostruct.* **8** (2013) 501
11. C. P. Bergmann, F. M. Machado, *Carbon Nanomaterials as Adsorbents for Environmental and Biological Applications*, Springer International Publishing, Cham, 2015, p. 105
12. Z. S. Veličković, A. D. Marinković, Z. J. Bajić, J. M. Marković, A. A. Perić-Grujić, P. S. Uskoković, M. D. Ristić, *Sep. Sci. Tech.* **48** (2013) 2047
13. K. A.Taleb, J. D. Rusmirović, M. P. Rančić, J. B. Nikolić, S. Ž. Drmanić, Z. S. Veličković, A. D. Marinković, *J. Serb. Chem. Soc.* **81** (2016) 1199
14. G. D. Vuković, A. D. Marinković, M. Čolić, M. Đ. Ristić, R. Aleksić, A. A. Perić-Grujić, P. S. Uskoković, *Chem. Eng. J.* **157** (2010) 238
15. J. Markovski, V. Marković, V. Đokić, M. Mitrić, M. Ristić, A. Onjia, A. Marinković, *Chem. Eng. J.* **237** (2014) 430
16. G. D. Vuković, A. D. Marinković, D. Obradović, V. Radmilović, M. Čolić, R. Aleksić, P. S. Uskoković, *Appl. Surface Sci.* **255** (2009) 8067
17. G. D. Vuković, A. D. Marinković, S. D. Škapin, M. Đ. Ristić, R. Aleksić, A. A. Perić-Grujić, P. S. Uskoković, *Chem. Eng. J.* **173** (2011) 855
18. D. Budimirović, Z.S. Veličković, R. V. Djokić, M. Milosavljević, J. Markovski, S. Lević, A. D. Marinković, *Chem. Eng. Res. Des.* **119** (2017) 75
19. S. E. Cabaniss, Environ. *Sci. Technol.* **45** (2011) 3202
20. J. Markovski, V. Đokić, M. Milosavljević, M. Mitrić, A. A. Perić-Grujić, A. Onjia, A. Marinković, *Ultrason. Sonochem.* **21** (2014) 790
21. A. Ntim and S. Mitra, *J. Chem. Eng. Data.* **56** (2011) 2077
22. J. C. Igwe, A. A. Abia, *Ecl. Quím., São Paulo* **32** (2007) 33
23. A. O Dada, A. P. Olalekan, A. M. Olatunya, O. Dada, *IOSR-JAC* **3** (2012) 38
24. M. A. Karimi and M. Kafi, *Arab. J. Chem.* **8** (2015) 812
25. S. Deniz, N. Tasci, E. K. Yetimoglu, M. V. Kahraman, *J. Serb. Chem. Soc.* **82** (2017) 215
26. S. Sarri, P. Misaelides, D. Zamboulis, F. Noli, J. Warchol, F. Pinakidou, M. Katsikini, *J. Serb. Chem. Soc.* **81** (2016) 1321
27. R. W. Peters and L. Shem, *Environ. Progr*. **11** (1992) 234.

(CC) 2017 SCS.